In situ isobaric lipid mapping by MALDI-ion mobility separation-mass spectrometry imaging

Tingting Fu, Janina Oetjen, Manuel Chapelle, Alexandre Verdu, Matthias Szesny, Arnaud Chaumot, Davide Degli Esposti, Olivier Geffard, Yohann Clément, Arnaud Salvador, et al.

Ayciriex Sophie (Orcid ID: 0000-0003-4813-5900)

Journal of Mass Spectrometry – Application Notes

Running head: MALDI-Ion mobility MS imaging for lipid mapping

In situ isobaric lipid mapping by MALDI-Ion Mobility Separation-Mass Spectrometry Imaging

Tingting Fu[1], Janina Oetjen[2], Manuel Chapelle[2], Alexandre Verdu[2], Matthias Szesny[2], Arnaud Chaumot[3], Davide Degli-Esposti[3], Olivier Geffard[3], Yohann Clément[1], Arnaud Salvador[1], Sophie Ayciriex[1]

[1]Univ Lyon, Université Claude Bernard Lyon 1, Institut des Sciences Analytiques, CNRS UMR 5280, 5 rue de la Doua, F-69100 Villeurbanne, France

[2]Bruker Daltonics GmbH, Fahrenheitstr. 4. D-28359 GmbH, Bremen, Germany

[3]INRAE, UR RiverLy, Laboratoire d'écotoxicologie, F-69625 Villeurbanne, France

Correspondence
Sophie Ayciriex, Université Claude Bernard Lyon 1, Institut des Sciences Analytiques, CNRS UMR 5280, 5 rue de la Doua, F-69100 Villeurbanne, France.
E-mail: sophie.ayciriex@univ-lyon1.fr

Abstract (max 100 words)

The highly diverse chemical structures of lipids make their analysis directly from biological tissue sections extremely challenging. Here we report the *in-situ* mapping and identification of lipids in a freshwater crustacean *Gammarus fossarum* using MALDI mass spectrometry imaging (MSI) in combination with an additional separation dimension using ion mobility spectrometry (IMS). The high-resolution trapped ion mobility spectrometry (TIMS) allowed efficient separation of isobaric/isomeric lipids showing distinct spatial distributions. The structures of the lipids were further characterized by MS/MS analysis. It is demonstrated that MALDI MSI with mobility separation is a powerful tool for distinguishing and localizing isobaric/isomeric lipids.

KEYWORDS

MALDI, ion mobility separation, TIMS, mass spectrometry imaging, lipid isomers

1. INTRODUCTION

Lipids are essential components which play critical structural, energy storage and signaling roles in living organisms[1]. Mass spectrometry-based lipidomics coupled with hyphenated techniques has become the key tool for depicting the constellation of lipid molecular species in cells, tissues as well as entire organisms. To access the diversity of a lipidome, specific extraction procedures based on usage of different organic solvents are applied. However, in this typical workflow, the spatial distribution of the measured molecular lipid species is lost. For over a decade, mass spectrometry imaging (MSI) has become the technique of choice to map multiple lipid species *in situ* and provide crucial information about their spatial localization[2]. Matrix assisted laser desorption/ionization (MALDI) MSI was initially developed for mapping proteins and peptides in tissue sections[3]. With the development of new matrices and progress in instrumentation[4], MALDI MSI is nowadays intensively employed, along with other MSI techniques notably secondary ion mass spectrometry (SIMS)[5, 6] and desorption electrospray ionization (DESI)[7, 8], for lipid mapping in biological and biomedical studies. However, due to the highly diverse lipid structures, one major challenge in MSI analysis is the separation of isomeric and isobaric lipid species sharing the same nominal mass-to-charge value. Ion mobility spectrometry is a gas phase separation technique which separates ions based on the form, size and charge of the ions and has shown great potential in resolving lipid isomers[9]. In addition to the classic drift tube ion mobility (DTIM)[10], various ion mobility separation methods including field asymmetric waveform IMS (FAIMS)[11], traveling wave IMS (TWIMS)[12] and more recently, trapped IMS (TIMS)[13] have been developed. IMS has now been commonly coupled to various mass spectrometers to provide additional separation dimension in addition to the chromatographic and mass separation, whereas its use in MSI especially MALDI MSI for differentiating isomeric lipids directly from tissue is less common and limited[14]. A few reports have shown that the coupling of IMS and MALDI MSI is beneficial in improving the detection and identification of lipids from tissue sections[15-19]. Among the different IMS techniques, TIMS has been shown a superior resolving power of ~400 in lipid analysis of human plasma[20]. Here we applied the recently developed timsTOF fleX MALDI MSI platform[19] to perform for the first time *in situ* mapping and identification of isobaric and isomeric lipids in the freshwater crustacean *Gammarus fossarum.*

2. MATERIALS AND METHODS

2.1 Reagents and materials

α-Cyano-4-hydroxycinamic acid (CHCA) was obtained from Bruker (Bremen, Germany). Unless otherwise specified, the solvents used were HPLC grade from Biosolve (Valkenswaard, Netherlands).

2.2 Tissue section preparation

Gammarus fossarum organisms were collected from a watercress population and acclimatized to laboratory conditions[21]. Female gammarids at an advanced reproductive stage of vitellogenesis were directly plunge-frozen in liquid N_2 and stored at -80 °C until cryo-sectioning[22]. Transverse sections were cut at -23 °C with a thickness of 12 µm utilizing a MICROM HM505E cryostat. The sections were immediately thaw mounted onto indium tin

oxide (ITO, Sigma-Aldrich) coated glass slides and dried for 30 min in a desiccator under low vacuum. Then the slides were placed in plastic bags filled with N_2 to avoid oxidation and stored at -80 °C until analysis.

2.3 Matrix coating

The tissue sections were coated with a homogeneous layer of matrix using a robotic TM-Sprayer (HTX Technologies, Chapel Hill, NC, USA) prior to MALDI imaging. 10 mg/mL CHCA solution prepared in ACN/H_2O/TFA (70:30:0.1, *v/v/v*) was used for positive ion mode MALDI MSI experiments. CHCA solution was sprayed at 70 °C with the following parameters: flow rate, 0.12 mL/min; nozzle height, 40 mm; nozzle moving speed, 120 cm/min; moving pattern, CC; track spacing, 3 mm; drying time, 30 s; nebulizing gas (N_2) pressure, 10 psi; 2 passes.

2.4 MALDI-IMS-MSI analysis

The gammarid tissue sections were imaged with a timsTOF fleX instrument (Bruker Daltonics, Bremen, Germany), of which a detailed description can be found in the reference 19. Briefly, the timsTOF fleX is a fully integrated timsTOF Pro instrument with a high-throughput, high-spatial resolution MALDI source and stage containing the SmartBeam 3D laser technology (Bruker Daltonics, Bremen, Germany)[23].

MALDI Imaging data in Q-TOF mode only and with trapped ion mobility switched-on were acquired in positive mode in the mass range of *m/z* 100-1000 with a spatial resolution of 20 µm. External mass calibration was performed with red phosphorous spotted next to the sections. For MALDI TIMS Imaging, ions were generated by 400 laser shots per pixel with a 10 kHz laser resulting in an accumulation time of 40 ms. Ions were separated and eluted in the second part of the dual TIMS device using a ramp time of 300 ms and a $1/K_0$ range of 0.6-1.8. Imaging data processing was performed with SCiLS Lab version 2020a. Ion mobility data was visualized with TIMS data viewer. The reduced ion mobility values ($1/K_0$) were converted to collisional cross section (CCS) values using the Mason-Schamp equation. When no MS/MS spectra were acquired, the mass to charge values were interrogated in open source database METLIN (https://metlin.scripps.edu/landing_page.php?pgcontent=mainPage) for tentative assignment.

2.5 Lipid extraction for lipidomics analysis

The gammarids (~ 20 mg wet weight) were homogenized in 300 µL 50 mM cold ammonium bicarbonate buffer with one stainless steel bead (Ø 4 mm). After centrifugation, 75 µL of supernatant was subjected to a modified lipid extraction protocol with MTBE (methyl tert-butyl ether). 700 µL of solvent mixture (MTBE/MeOH, 7:1, *v/v*) containing a mix of synthetic internal standard representative for each lipid class was added (25 µL of Splash® LIPIDOMIX® Mass Spec Standards, Avanti Polar Lipids). Samples were vortexed for 1h at 4 °C. Phase separation was produced by adding 200 µL of water and agitating for 15 min at 4 °C, followed by centrifugation (15 min, 13 400 rpm at 4 °C). The upper organic phase (600 µL) was collected, dried down under nitrogen and reconstituted in 20 µL (CH_2Cl_2/MeOH, 1:1, *v/v*) and 180 µL (IPA/ACN/H_20, 2:1:1, *v/v/v*) for LC-MS/MS analysis.

2.6 ESI-IMS-MS analysis

For lipidomics analysis, the lipid extract was separated on a Bruker Elute UHPLC system using a Bruker Intensity Solo 2 C18 column (100×2.1 mm, 1.8 µm). The column temperature was set to 55 °C. Solvent A was composed of ACN/H_2O (60:40, *v/v*) with 0.1% formic acid and 1 mM ammonium formate. Solvent B was composed of IPA/ACN (90:10, *v/v*) with 0.1% formic acid and 1 mM ammonium formate. The flow rate was set to 0.4 mL/min. 5 µL of the sample was injected. The 20 min LC-gradient started with 40% solvent B and was increased in the following way: 2 min, 43%; 2.1 min, 50%; 12 min, 54%; 12.1 min, 70%; 18 min, 99%, 18.1 min, 40%, 20 min, 40% solvent B. The LC system was coupled to a timsTOF Pro instrument with ESI source (Bruker Daltonics, Bremen, Germany) essentially as described [24]. Briefly, ions were detected in positive ion mode in the mass range of *m/z* 100-1300 using PASEF technology [23, 25]. Tune Mix (Agilent, Santa Clara, CA) was used for TIMS calibration.

3. RESULTS AND DISCUSSION

3.1 Imaging isobaric/ isomeric lipid species by MALDI-IMS-MSI

Female *G. fossarum* is typically ~1 cm in length. All the main organs of this organism including muscle, oocytes, hepatopancreas (HP), intestine, as well as the ventral pouch (VP) with embryos can be readily recognized in the transverse section which is 2-3 mm in length and width (FIGURE 1A). With TIMS activated, MALDI MSI was performed with a pixel size of 20 µm which could unambiguously resolve the various organs of this tiny organism while providing good sensitivity for lipid detection from the tissue section. With the obtained mass resolution of 60 000 at *m/z* 782.561, a considerable amount of ion species with different $1/K_0$values were not separated in the *m/z* dimension (FIGURE S3), indicating richer molecular information can be generated with IMS compared to current routine MALDI experiments. As illustrated in FIGURE 1, the heat map representation of the *m/z* and mobility data shows that there are two conformations corresponding to the same *m/z* value of 782.561. The reconstructed ion image of the major conformation with $1/K_0 = 1.426 \pm 0.01$ (CCS = 290.7 $Å^2$) exhibits its predominant distribution in the muscle of the female gammarid, whereas the minor conformation with $1/K_0 = 1.402 \pm 0.01$ (CCS = 285.7 $Å^2$) is found to be more abundant in the oocytes and hepatopancreas. More examples illustrating the ion mobility separation of isobaric/isomeric lipid species with different spatial distributions can be found in the supplementary information (FIGURE S4-S6). Thus, the incorporation of IMS helped to avoid misleading visualization, as the combined ion image represents the spatial distribution of the two or more ion species.

3.2 MS/MS characterization of the isobaric/ isomeric lipid species

To go further into the characterization of the aforementioned isobaric/isomeric species exhibiting distinct distributions at *m/z* 782.56, *in situ* MS/MS analysis was performed on the gammarid tissue section. From the muscle region as shown in FIGURE 1A, the MALDI TOF MS/MS spectrum of the precursor ion at *m/z* 782.57 was acquired via CID with collision energy set at 45 eV (FIGURE 2). The ion at *m/z* 184 corresponding to phosphocholine is a characteristic fragment of lipid species phosphatidylcholine (PC) and sphingomyelin. According to the nitrogen rule, the precursor ion is attributed as a PC species given that it

possesses an even nominal mass. The prominent fragment ions at *m/z* 577 and 599 indicate that the isolated lipid molecule is a sodium adduct species. Finally, the fragment ions at *m/z* 239 and 265 suggest the two fatty acid chains of the PC species are C16:0 and C18:1, respectively. Note that the regiolocalization of the double bonds and the fatty acid moieties on the glycerol backbone of the phospholipid are not determined. Therefore, the main component of the detected ion at *m/z* 782.57 is attributed as sodium adduct of PC 16:0-18:1, which is further validated by the fragments produced at *m/z* 441-504. The comparison of the experimental CCS value of PC 16:0-18:1 to the one reported in the literature (PC 34:1, CCS~292 $Å^2$) confirmed the attribution[26]. The minor component of the ion species with same *m/z* value was not characterized directly from the tissue due to its low abundance but was successfully assigned by LC-ESI-MS/MS analysis of the lipid extract of this organism with the same instrument. The extracted MS/MS spectra of the precursor ion at *m/z* 782.57 suggested the presence of two more conformations sharing the same *m/z* value, namely protonated PC 18:1-18:3 and protonated PC 16:0-20:4 (FIGURE S2).

3.3 Lipid composition in different organs of female *G. fossarum*

In order to examine the lipid species in different organs of female gammarid *G. fossarum*, three regions of interest (ROIs) representing respectively oocytes, dorsal muscle and hepatopancreas were drawn and the ions colocalizing to each region were generated using the function 'find co-localized *m/z* values' in SCiLS (version 2020a). FIGURE 3 displays images of the five most abundant ions specifically colocalizing to the corresponding organs. The tentatively assigned ether PC molecular species (*m/z* 766.574, $[PC(O\text{-}16:0/20:5)+H]^+$/$[PC(P\text{-}16:0/20:4)+H]^+$; *m/z* 792.590, $[PC(O\text{-}16:0/22:6)+H]^+$/$[PC(P\text{-}16:0/22:5)+H]^+$; *m/z* 794.606, $[PC(O\text{-}16:0/22:5)+H]^+$/$[PC(P\text{-}16:0/22:4)+H]^+$ and its isotopic peak at *m/z* 795.607) turned out to be characteristic lipid species in the oocytes of the female gammarid. The enrichment of ether PC molecular species specifically distributed in oocytes could have a potential active role in the metabolism during oocyte maturation and development[27]. Lipids belonging to various families were detected in the muscle tissue such as *m/z* 772.525, $[PC(32:0)+K]^+$ (and the isotopic peak at *m/z* 773.530); *m/z* 834.679, $[GlcCer(d18:1/24:0)+Na]^+$ and *m/z* 883.678, $[TAG(53:8)+Na]^+$. Hepatopancreas (HP) is the digestive gland in gammarids, thus, it is not surprising that ions colocalized in HP were also found in the intestine as shown in FIGURE 3C. These ions were not assigned, and they were probably exogenous compounds uptaken from the environment. The three-color overlay of ions at *m/z* 794.606, *m/z* 772.525 and *m/z* 375.065 illustrated the specific distributions of different chemical species in the organs of female *G. fossarum* and demonstrated the capability of high resolution MALDI imaging in resolving fine tissue structures in a very small sample.

4. CONCLUSIONS

In situ mapping and identification of isobaric and isomeric lipid species in crustacean *G. fossarum* were achieved by MALDI MSI coupled with ion mobility separation. Distinct distribution of the isobaric lipid species at *m/z* 782.561 were observed in the muscle and oocytes of the female gammarid, respectively. It was revealed by combining ESI-IMS MS/MS and MALDI- MS/MS analyses that the ion at *m/z* 782.561 were composed of three isobaric and isomeric species: $PC(16:0\text{-}18:1)+Na^+$, $PC(18:1\text{-}18:3)+H^+$, and $PC(16:0\text{-}20:4)+H^+$. Moreover,

the generation of ion species colocalizing to specific organs disclosed different lipid composition and abundance in muscle, hepatopancreas and oocytes in the female gammarid. Overall, we demonstrated that this particular MALDI-IMS-MSI approach is highly beneficial for localizing and characterizing isomeric and isobaric lipid species that are potentially involved in different biofunctions.

ACKNOWLEDGEMENTS

This work was supported by the Agence Nationale de la Recherche (grant number: ANR-18-CE34-0008). The authors thank Nicolas Delorme for technical assistance in gammarids sampling as well as Khedidja Abbaci for the input of gammarid anatomy.

Conflict of interest

The authors declare the following conflict of interest: JO, MC, AV and MS are employed at Bruker Daltonics GmbH.

ORCID

Tingting Fu https://orcid.org/0000-0003-0050-9571

Janina Oetjen https://orcid.org/0000-0002-4088-5742

Arnaud Chaumot https://orcid.org/0000-0001-9132-3419

Davide Degli-Esposti https://orcid.org/0000-0003-1390-4845

Olivier Geffard https://orcid.org/0000-0001-7760-4644

Yohann Clément https://orcid.org/0000-0002-9852-2856

Arnaud Salvador https://orcid.org/0000-0002-5981-3028

Sophie Ayciriex https://orcid.org/0000-0003-4813-5900

REFERENCES

1. van Meer, G.; Voelker, D. R.; Feigenson, G. W., Membrane lipids: where they are and how they behave. *Nat Rev Mol Cell Biol* **2008,** *9* (2), 112-24.

2. Gode, D.; Volmer, D. A., Lipid imaging by mass spectrometry–a review. *Analyst* **2013**.

3. Caprioli, R. M.; Farmer, T. B.; Gile, J., Molecular imaging of biological samples: localization of peptides and proteins using MALDI-TOF MS. *Anal Chem* **1997,** *69* (23), 4751-60.

4. Baker, T. C.; Han, J.; Borchers, C. H., Recent advancements in matrix-assisted laser desorption/ionization mass spectrometry imaging. *Curr Opin Biotechnol* **2017,** *43*, 62-69.

5. Bich, C.; Touboul, D.; Brunelle, A., Cluster TOF-SIMS imaging as a tool for micrometric histology of lipids in tissue. *Mass Spectrom Rev* **2014,** *33* (6), 442-51.

6. Passarelli, M. K.; Winograd, N., Lipid imaging with time-of-flight secondary ion mass spectrometry (ToF-SIMS). *Biochim Biophys Acta* **2011,** *1811* (11), 976-90.

7. Banerjee, S.; Zare, R. N.; Tibshirani, R. J.; Kunder, C. A.; Nolley, R.; Fan, R.; Brooks, J. D.; Sonn, G. A., Diagnosis of prostate cancer by desorption electrospray ionization mass spectrometric imaging of small metabolites and lipids. *Proc Natl Acad Sci U S A* **2017,** *114* (13), 3334-3339.

8. Eberlin, L. S.; Ferreira, C. R.; Dill, A. L.; Ifa, D. R.; Cooks, R. G., Desorption electrospray ionization mass spectrometry for lipid characterization and biological tissue imaging. *Biochim Biophys Acta* **2011,** *1811* (11), 946-60.

9. Hinz, C.; Liggi, S.; Griffin, J. L., The potential of Ion Mobility Mass Spectrometry for high-throughput and high-resolution lipidomics. *Curr Opin Chem Biol* **2018,** *42*, 42-50.

10. Eiceman, G. A., *Advances in ion mobility spectrometry: 1980-1990*. 1991; Vol. 22, p 471-490.

11. Purves, R. W.; Guevremont, R., Electrospray ionization high-field asymmetric waveform ion mobility spectrometry-mass spectrometry. *Anal Chem* **1999,** *71* (13), 2346-57.

12. Shvartsburg, A. A.; Smith, R. D., Fundamentals of traveling wave ion mobility spectrometry. *Anal Chem* **2008,** *80* (24), 9689-99.

13. Fernandez-Lima, F.; Kaplan, D. A.; Suetering, J.; Park, M. A., Gas-phase separation using a trapped ion mobility spectrometer. *Int J Ion Mobil Spectrom* **2011,** *14* (2-3).

14. Sans, M.; Feider, C. L.; Eberlin, L. S., Advances in mass spectrometry imaging coupled to ion mobility spectrometry for enhanced imaging of biological tissues. *Curr Opin Chem Biol* **2018,** *42*, 138-146.

15. Chughtai, K.; Jiang, L.; Greenwood, T. R.; Glunde, K.; Heeren, R. M., Mass spectrometry images acylcarnitines, phosphatidylcholines, and sphingomyelin in MDA-MB-231 breast tumor models. *J Lipid Res* **2013,** *54* (2), 333-44.

16. Jackson, S. N.; Barbacci, D.; Egan, T.; Lewis, E. K.; Schultz, J. A.; Woods, A. S., MALDI-Ion Mobility Mass Spectrometry of Lipids in Negative Ion Mode. *Anal Methods* **2014,** *6* (14), 5001-5007.

17. Jackson, S. N.; Ugarov, M.; Egan, T.; Post, J. D.; Langlais, D.; Albert Schultz, J.; Woods, A. S., MALDI-ion mobility-TOFMS imaging of lipids in rat brain tissue. *J Mass Spectrom* **2007,** *42* (8), 1093-8.

18. McLean, J. A.; Ridenour, W. B.; Caprioli, R. M., Profiling and imaging of tissues by imaging ion mobility-mass spectrometry. *J Mass Spectrom* **2007,** *42* (8), 1099-105.

19. Spraggins, J. M.; Djambazova, K. V.; Rivera, E. S.; Migas, L. G.; Neumann, E. K.; Fuetterer, A.; Suetering, J.; Goedecke, N.; Ly, A.; Van de Plas, R.; Caprioli, R. M., High-Performance Molecular Imaging with MALDI Trapped Ion-Mobility Time-of-Flight (timsTOF) Mass Spectrometry. *Anal Chem* **2019,** *91* (22), 14552-14560.

20. Jeanne Dit Fouque, K.; Ramirez, C. E.; Lewis, R. L.; Koelmel, J. P.; Garrett, T. J.; Yost, R. A.; Fernandez-Lima, F., Effective Liquid Chromatography-Trapped Ion Mobility Spectrometry-Mass Spectrometry Separation of Isomeric Lipid Species. *Anal Chem* **2019,** *91* (8), 5021-5027.

21. Gouveia, D.; Chaumot, A.; Charnot, A.; Queau, H.; Armengaud, J.; Almunia, C.; Salvador, A.; Geffard, O., Assessing the relevance of a multiplexed methodology for proteomic biomarker measurement in the invertebrate species Gammarus fossarum: A physiological and ecotoxicological study. *Aquat Toxicol* **2017,** *190*, 199-209.

22. Geffard, O.; Xuereb, B.; Chaumot, A.; Geffard, A.; Biagianti, S.; Noel, C.; Abbaci, K.; Garric, J.; Charmantier, G.; Charmantier-Daures, M., Ovarian cycle and embryonic development in Gammarus fossarum: application for reproductive toxicity assessment. *Environ Toxicol Chem* **2010,** *29* (10), 2249-59.

23. Meier, F.; Brunner, A. D.; Koch, S.; Koch, H.; Lubeck, M.; Krause, M.; Goedecke, N.; Decker, J.; Kosinski, T.; Park, M. A.; Bache, N.; Hoerning, O.; Cox, J.; Rather, O.; Mann, M., Online Parallel Accumulation-Serial Fragmentation (PASEF) with a Novel Trapped Ion Mobility Mass Spectrometer. *Mol Cell Proteomics* **2018,** *17* (12), 2534-2545.

24. Vasilopoulou, C. G.; Sulek, K.; Brunner, A. D.; Meitei, N. S.; Schweiger-Hufnagel, U.; Meyer, S. W.; Barsch, A.; Mann, M.; Meier, F., Trapped ion mobility spectrometry and PASEF enable in-depth lipidomics from minimal sample amounts. *Nat Commun* **2020,** *11* (1), 331.

25. Meier, F.; Beck, S.; Grassl, N.; Lubeck, M.; Park, M. A.; Raether, O.; Mann, M., Parallel Accumulation-Serial Fragmentation (PASEF): Multiplying Sequencing Speed and Sensitivity by Synchronized Scans in a Trapped Ion Mobility Device. *J Proteome Res* **2015,** *14* (12), 5378-87.

26. Leaptrot, K. L.; May, J. C.; Dodds, J. N.; McLean, J. A., Ion mobility conformational lipid atlas for high confidence lipidomics. *Nat Commun* **2019,** *10* (1), 985.

27. Bertevello, P. S.; Teixeira-Gomes, A. P.; Seyer, A.; Vitorino Carvalho, A.; Labas, V.; Blache, M. C.; Banliat, C.; Cordeiro, L. A. V.; Duranthon, V.; Papillier, P.; Maillard, V.; Elis, S.; Uzbekova, S., Lipid Identification and Transcriptional Analysis of Controlling Enzymes in Bovine Ovarian Follicle. *Int J Mol Sci* **2018,** *19* (10).

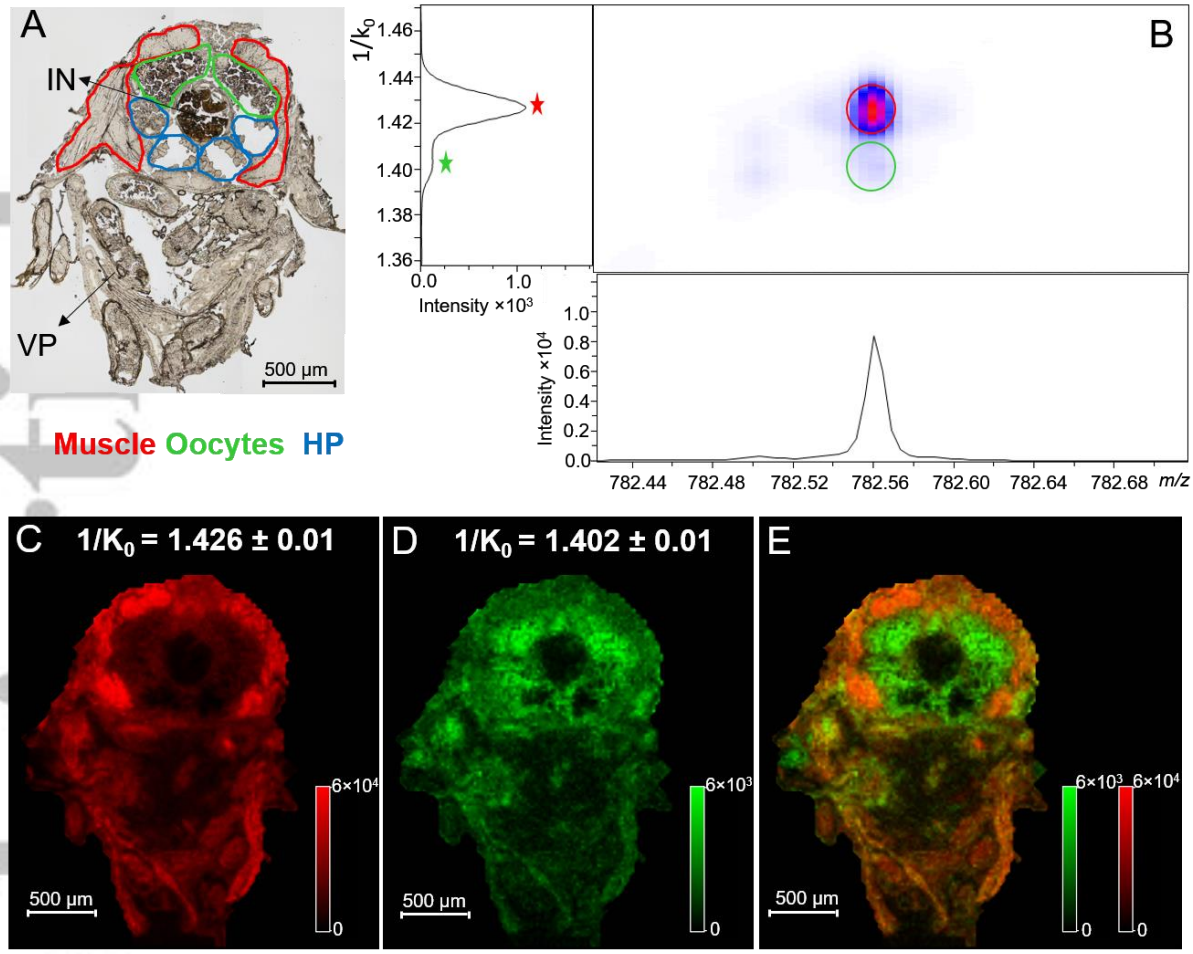

FIGURE 1 MALDI-IMS-MSI of female *G. fossarum* tissue section. A. Optical image of the tissue section analysed by MALDI-IMS-MSI and washed with EtOH to remove the CHCA matrix. HP: hepatopancreas; In: Intestine. VP: ventral pouch. B. Ion mobility separation of two ion species with the same *m/z* value of 782.561. C. Ion image of the ion at *m/z* 782.561 with $1/K_0 = 1.426 \pm 0.01$(CCS = 290.7 Å^2). D. Ion image of ion at *m/z* 782.561 with $1/K_0 = 1.402 \pm 0.01$ (CCS = 285.7 Å^2). E. Two-colour overlay of ion images of the two isobaric species.

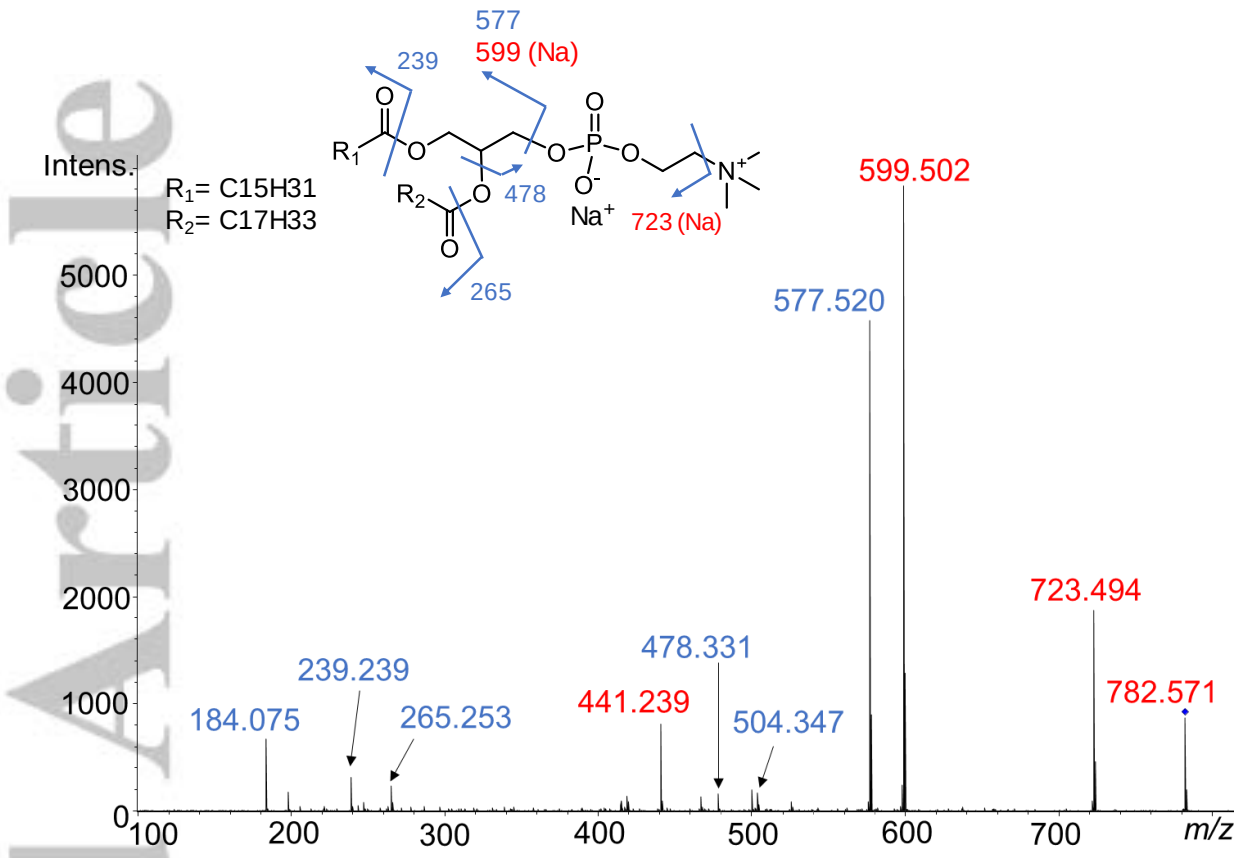

FIGURE 2 MALDI MS/MS spectrum of the precursor ion at *m/z* 782.571 from tissue section of female *G. fossarum*. *m/z* values highlighted in red in the spectrum correspond to sodiated ions.

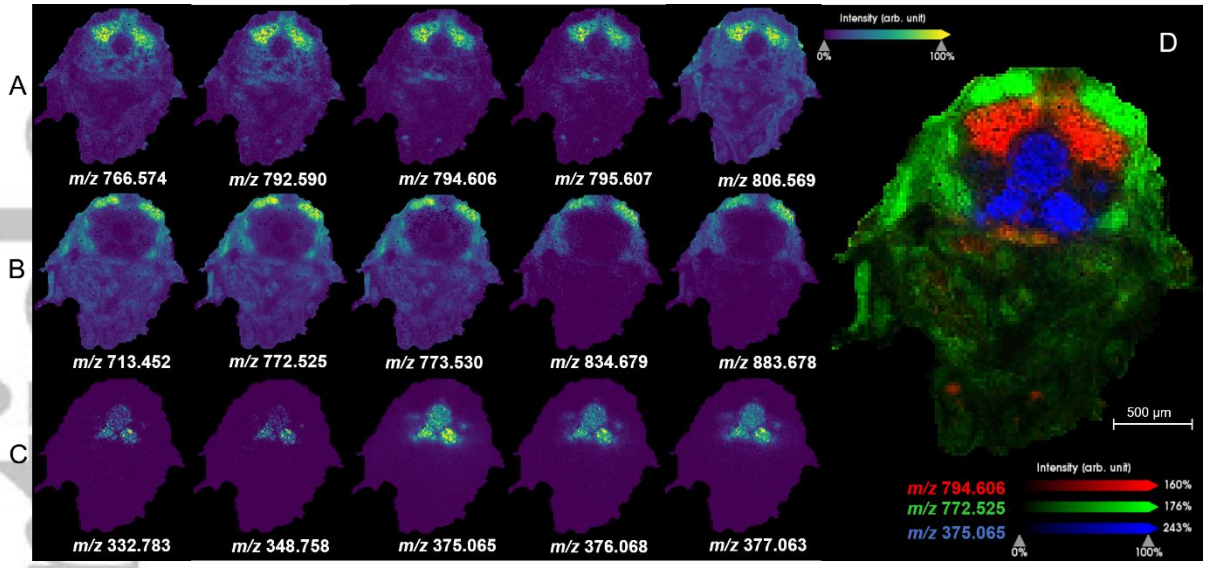

FIGURE 3 Representative lipid species in different organs of *G. fossarum*. A-C: ion images of lipid species colocalizing in oocytes (A), muscle (B) and hepatopancreas (C), respectively. D. Three-color overlay of ions at *m/z* 794.606 (red), *m/z* 772.525 (green) and *m/z* 375.065 (blue).